Met.O.871
METEOROLOGICAL OFFICE

the meteorological magazine

SEPTEMBER 1974 No 1226 Vol 103
Her Majesty's Stationery Office

METEOROLOGICAL OFFICE Met.O.871

THE METEOROLOGICAL MAGAZINE

Vol. 103, No. 1226, September 1974

551·554

A SCHEME FOR DERIVING DAY-TIME BOUNDARY-LAYER WIND PROFILES

By F. B. SMITH and D. J. CARSON

Summary. This scheme for deriving day-time boundary-layer wind profiles uses readily available parameters, namely: time of day, month, cloud amount, surface geostrophic wind and surface wind. The scheme allows for the effects of surface roughness, stability and diurnal and seasonal variations in boundary-layer depth. Typical profiles for both rural and urban sites are derived.

The scheme is illustrated fully by example in the section on 'Application', which may be read independently of the theoretical background which is outlined in the previous section. An extension of the basic scheme to allow for thermal-wind effects is described.

Introduction. This paper describes a scheme for estimating the mean wind-speed profile in a day-time atmospheric boundary layer in terms of the following parameters: time of day, month, cloud amount, the surface geostrophic wind speed and the mean 10-metre wind speed measured by a properly exposed anemometer. At times it may be necessary to replace the surface geostrophic wind by the gradient wind if the air trajectories have significant curvature or to adjust its value to allow for thermal wind effects which, on occasions, can be very important throughout the boundary layer.

The scheme takes account of boundary-layer stability and surface roughness in determining the nature of the wind profile in the lowest few tens of metres and also allows for diurnal and seasonal variations in the depth of the boundary layer which affect the way in which the wind speed approaches the 'free-stream' value (the geostrophic- or gradient-wind value) at the top of the boundary layer.

Two categories of profile are illustrated according to the surface roughness of the terrain over which the profile is to be estimated. One may be classed as a rural profile at the site of the anemometer set within typical English countryside (i.e. above a well-maintained level grass surface surrounded at a reasonable distance by hedges, trees, villages etc.); the other is for use over an urban or forested area.

The second section gives the theoretical background to the basic scheme with reference to source material. The third section gives the procedure for applying the scheme and indicates its limitations. A worked example is also given and this section can be read without reference to the other sections. A further section describes how the thermal wind can be incorporated into the scheme when it is important.

Theoretical background

Parameters needed to specify the profiles. Straightforward formulations of the wind profile throughout the whole of the boundary layer do not exist. The composite profiles presented here are obtained from a combination of the wind profile based on standard similarity-theory arguments applying well below the top of the boundary layer, the height of the boundary layer and the magnitude of the 'free-stream' wind at the top.

The parameters needed to specify the whole profile are:

(a) z_0, the surface roughness. The effective z_0 generally varies from one part of the wind profile to another. For the near-surface profile the very local nature of the surface (e.g. short grass) at the site is important but away from the ground z_0 represents an average roughness over an upwind area which is significantly affecting the wind profile at the height concerned. Since at greater heights the effective z_0 will have to take into account hedges, copses, buildings etc. it will generally be greater than the z_0 used closer to the ground.

Four values of z_0 have been used to determine the final composite profiles. At the rural site, assumed to be a typical meteorological observing station, z_0 is assumed 3 cm close to the surface, $z_0 = 10$ cm in a layer containing the anemometer at 10 metres and $z_0 = 30$ cm above about 100 metres, as a typical z_0 for varied English countryside. For the urban profile, which is only applicable at heights well above the height of the roughness elements themselves, $z_0 = 1$ m is taken from about 20 metres merging once more into the profiles for $z_0 = 30$ cm at heights in excess of 100 metres where the urban environment will no longer significantly affect the profile unless the city extends for more than a few kilometres upwind.

(b) Some measure of the degree of instability in the surface stress layer.

(c) The total incoming short-wave radiation, R.

(d) The depth, h, of the atmospheric boundary layer.

(e) The value of the 10-metre wind speed, u_{10}, corresponding to a surface roughness $z_0 = 10$ cm or, alternatively, the surface geostrophic wind (V_g) or gradient wind (V_{gr}).

A stability parameter in common use in the surface stress layer is the surface Monin–Obukhov length, L, defined by

$$L = \frac{-u_*^3 \rho c_p T}{gkH},$$

where u_* is the surface friction velocity, ρ is the mean density of the air, c_p is the specific heat of air at constant pressure, T is the mean absolute temperature of the air, g is the acceleration due to gravity, k is the von Kármán constant and H is the surface sensible heat flux which is assumed closely related to the incoming solar radiation, R. From his model for boundary-layer profiles in unstable conditions, Smith[1] produced curves of u_*/V_g as a function of the surface Rossby number, V_g/fz_0 (where f is the Coriolis parameter), and a stability parameter, H/V_g^2. Also, knowing u_z/u_* as a function of z, L and z_0 for the surface layers, Smith provided curves showing the interrelationships between R, V_g, u_*, L, $u_{10}(z_0)$ and z_0. By use of these relationships it is found that the parameter $V_g/u_{10}(z_0)$ can be represented, to a high degree of approximation, as a function of z_0 and L only and can therefore be used as a stability

parameter in place of L, for any given z_0. For $z_0 = 10$ cm, $V_g/u_{10} = 2.0$ corresponds, in the absence of thermal-wind effects, to neutral stability, 1.75 to $L \approx -100$ m and 1·5 to $L \approx -10$ m.

A further result from Smith's curves is that the wind speed $u_{10}(z_0)$ at 10 metres corresponding to a surface roughness z_0 is proportional to the wind speed u_{10} at 10 metres corresponding to a surface roughness of 10 cm, *under the same external conditions of R and* V_g. The constant of proportionality is, to a good approximation, independent of the Monin–Obukhov length, L. In particular:

$$\frac{u_{10}(z_0)}{u_{10}} \approx r(z_0) = \begin{cases} 0{\cdot}86 \text{ for } z_0 = 0{\cdot}3 \text{ m}, \\ 0{\cdot}73 \text{ for } z_0 = 1{\cdot}0 \text{ m}. \end{cases}$$

The new stability parameter $V_g/u_{10}(z_0)$ is therefore readily replaced in the analysis by V_g/u_{10}.

The presentation of the profiles is greatly simplified by these observations and the format

$$\frac{u_z}{u_{10}} = f(z, z_0, V_g/u_{10}, h)$$

is adopted, where z_0 is a function of height reflecting the upwind variations in surface roughness, as discussed above.

Determination of the stability parameter V_g/u_{10}. In some situations both u_{10} and V_g will be known from anemometer readings and synoptic charts. The stability parameter V_g/u_{10} will then be known directly. In areas of complex topography this may be the only acceptable way of proceeding. Otherwise one or other of u_{10} and V_g must be available and can be used together with the incoming solar radiation, R, to deduce the stability parameter. However, R is not generally readily available but can be estimated from three easily assessed parameters, namely the time of day, the month and the cloud amount. Figures 1 and 2, based on four years of radiation data from Cambridge, show the dependence of R on the three parameters. A value of R for 0–1 oktas of cloud is estimated from Figure 1 and is modified for the actual cloud amount from Figure 2. The derivation of these figures, first used by Smith *et alii*,[2] is based on information on the Cambridge radiation data discussed and displayed in Smith and Jeffrey.[3]

Figure 3 represents V_g/u_{10} as a function of R and u_{10} and is derived as a direct consequence of Smith's[1] curves and the inferred relationship between V_g/u_{10} and L. Alternatively V_g/u_{10} can be represented as a function of R and V_g by the directly related Figure 4.

Figures 1, 2 and 3 (or 4) provide then the stability parameter V_g/u_{10} which will be used in the classification of the profiles.

The wind profile in the surface stress layer. The wind profile in the surface stress layer is determined from the Monin-Obukhov similarity theory formulation,

$$\frac{\partial u}{\partial z} = \frac{u_*}{kz}\,\varphi_m(z/L),$$

where, following Businger[4] and Dyer and Hicks,[5] $\varphi_m(z/L)$ for neutral and unstable conditions is given by

$$\varphi_m(z/L) = (1-16\,z/L)^{-\frac{1}{4}}, \; |\,z/L\,| \leqslant 1.$$

After integration this gives

$$\frac{u_z}{u_{10}(z_0)} = \frac{\chi(\xi_z)-\chi(\xi_{z,0})}{\chi(\xi_{10})-\chi(\xi_{z,0})}$$

$$\approx \frac{u_z}{r(z_0)u_{10}},$$

where

$$\chi(\xi_z) = \ln\left[\frac{\xi_z-1}{\xi_z+1}\right] + 2\tan^{-1}\xi_z$$

and

$$\xi_z = (1-16\,z/L)^{\frac{1}{4}}.$$

The low-level profiles were determined in this way with V_g/u_{10} used as the stability parameter for classification purposes.

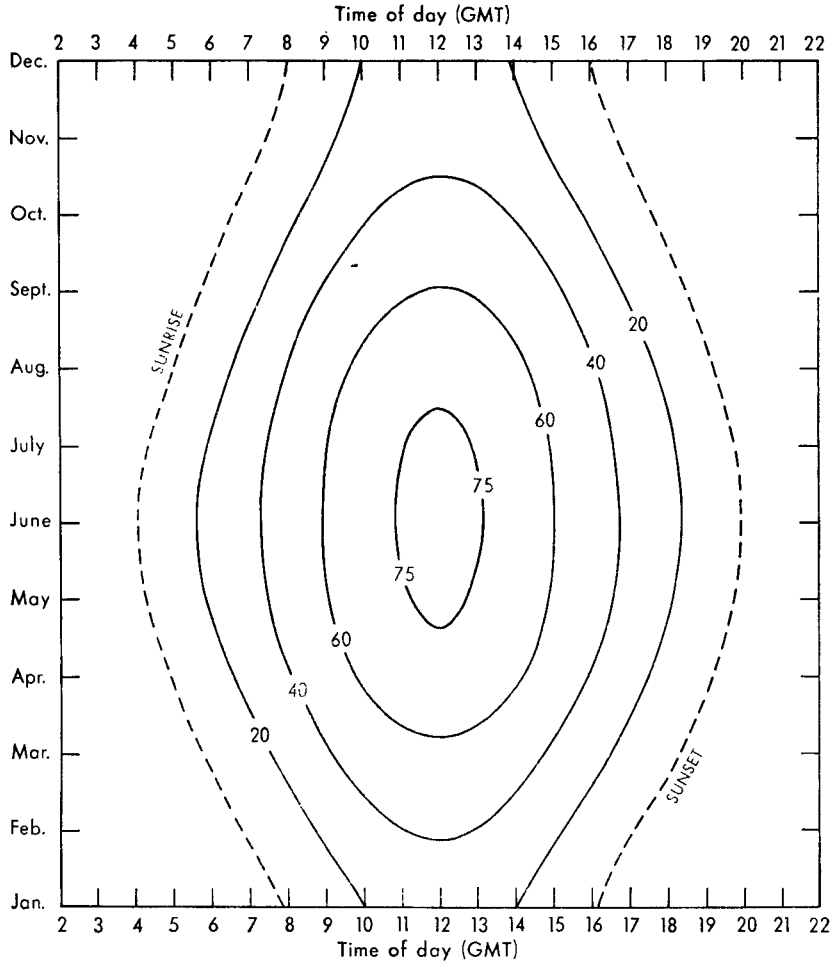

FIGURE 1—INCOMING SOLAR RADIATION, R_0, IN MILLIWATTS PER SQUARE CENTIMETRE FOR 0–1 OKTA OF CLOUD

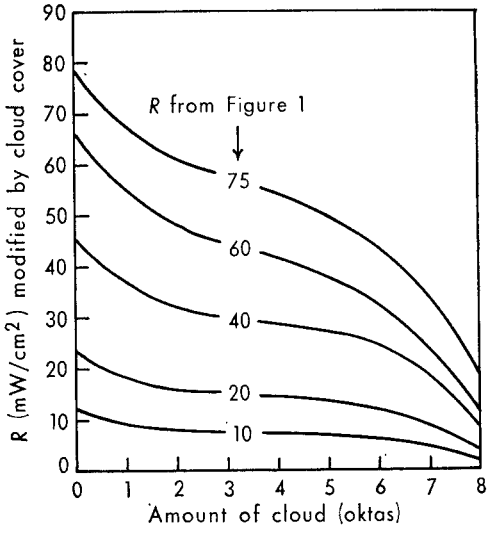

FIGURE 2—INCOMING SOLAR RADIATION MODIFIED BY CLOUD COVER
As deduced from unmodified value R_0 from Figure 1.

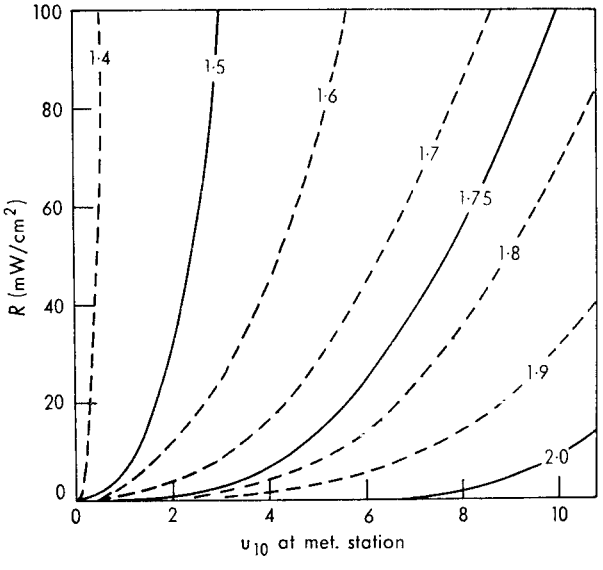

FIGURE 3—CONTOURS OF V_g/u_{10} IN TERMS OF R AND u_{10}
Values of u_{10} are in metres per second.

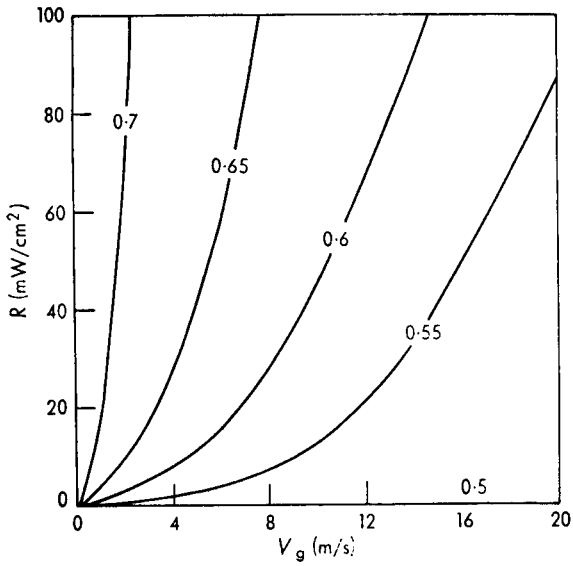

FIGURE 4—CONTOURS OF u_{10}/R IN TERMS OF R AND V_g

The wind profile above the surface stress layer. To determine the wind profile from the top of the surface stress layer to the top of the boundary layer we use the two parameters V_g/u_{10} and h and assume that the wind speed will attain the 'free-stream' value V_g at $z = h$.

The value V_g/u_{10} is obtained either directly or by the procedure described above.

To obtain a reliable estimate of h is not an easy task. There are, generally speaking, no estimates of this depth readily available, although radiosonde ascents might be used with caution to provide an estimate at certain times. It should be noted that formulae based on the steady-state similarity approach applied to the whole layer are only of use for estimating h if the boundary layer is neutral and has been so for some time. Such formulae are quite inadequate for use with the generally non-steady, diabatic boundary layer. This is because the depth is determined by mechanical mixing and the total amount of heat which has entered the layer, not just the heat received at any instant.

The determination of h, in the absence of any direct information, has been somewhat simplified and reduced to the nomogram of Figure 5. Here h is determined as a function of time of day, month, cloud amount and the wind speed at 10 metres at the meteorological station site (i.e. 10 cm is the effective surface roughness for the profile at 10 m). The curves are based on the developing boundary-layer model of Carson[6] which has been used with mean boundary-layer temperature profiles obtained by Hardy (private communication) from a study of Balthum ascents at Cardington over a period of 10 years. This type of approach was first developed for a practical scheme, designed and discussed by Smith,[7] for estimating the vertical dispersion of a plume from a source near ground-level. Here we have extended the basic model to allow for a contribution to h due to mechanically, as opposed to thermally, generated turbulent mixing.

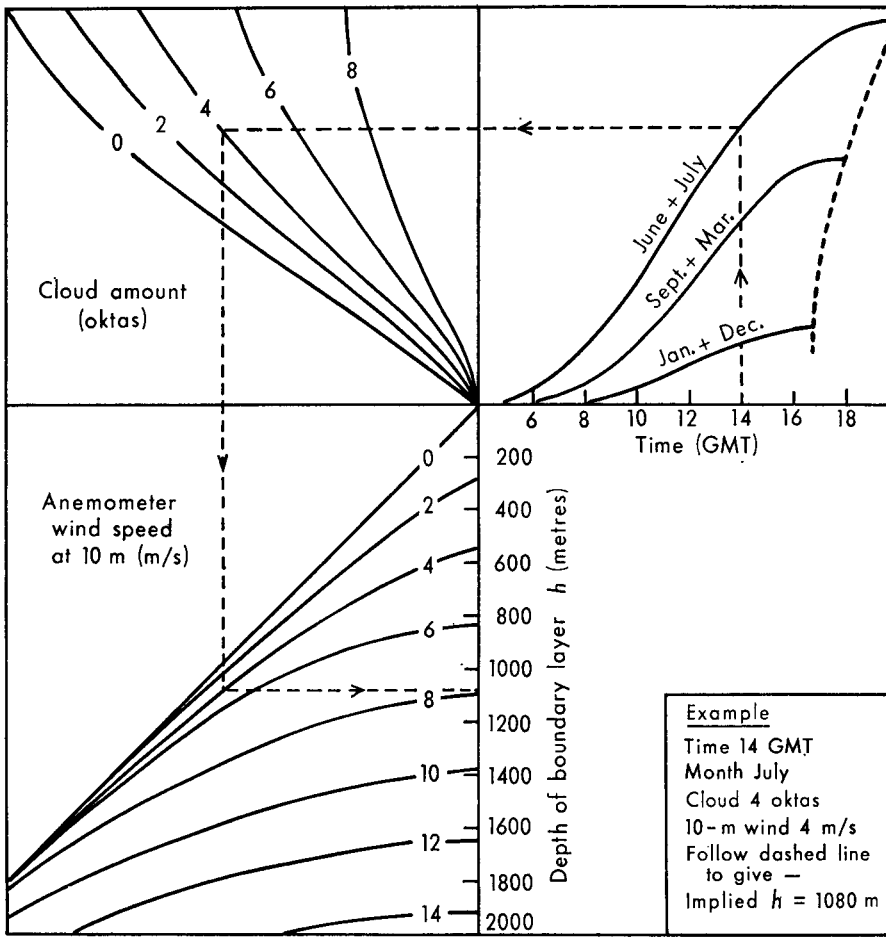

FIGURE 5—NOMOGRAM FOR THE DETERMINATION OF THE DEPTH OF THE BOUNDARY LAYER, h

Knowing the height h at which u_z/u_{10} attains the derived value V_g/u_{10} it is necessary to carry a somewhat subjective extrapolation of the low-level profile for $z_0 = 30$ cm to meet this upper-boundary condition.

Finally a matching process has to take place between the profiles for the three values of z_0. The profile for $z_0 = 3$ cm is given most weight in the first few metres, appropriate to the surrounding grass-covered area. At 10 metres the actual anemometer wind, u_{10}, gives a fixed point and account is taken of the slope of the profile there corresponding to $z_0 = 10$ cm. Above about 100 metres the composed profile for $z_0 = 30$ cm described in the previous paragraph is given greatest weight, appropriate to the effect of distant, more severe, roughness. Naturally there is a further element of subjectivity in this matching process but with so many fixed constraints (the value of z_0 at the ground, u_{10}, h etc.) the expected errors arising from this are really quite small.

Over an urban area the matching process blends the profile for $z_0 = 1$ m below 100 metres into the derived profile for $z_0 = 30$ cm above about 100 metres. Note that the urban profile cannot have meaning below about twice the typical building height.

These profiles are presented in Figure 6 for several values of V_g/u_{10} and h.

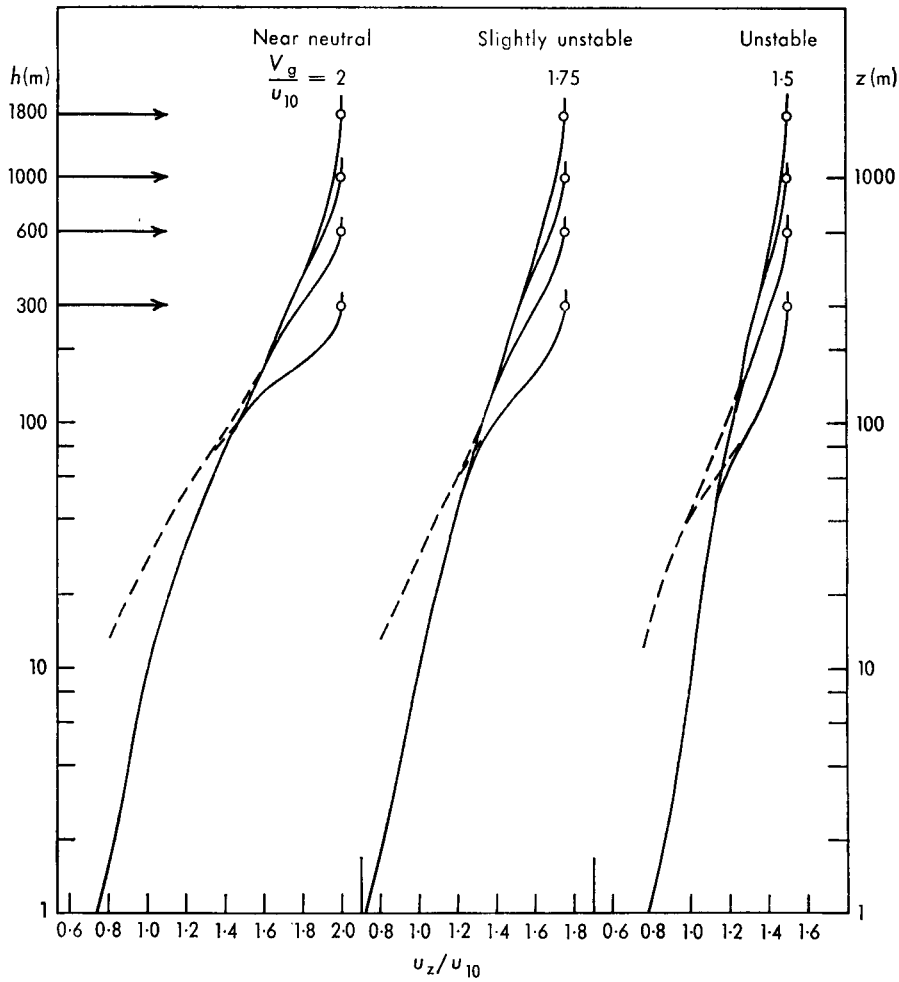

FIGURE 6—EXAMPLES OF WIND PROFILES

Below 100 metres pecked lines denote urban profile and continuous lines the profile at meteorological stations.

The application of the scheme. This section describes how to use the scheme without reference to the theoretical background given above. To clarify the process an actual example will be followed step by step; the example assumes the following conditions:

(a) Time: 14 GMT; month: July; place: a typical meteorological observing station in central England, set in the country.

(b) Cloud amount has been fairly steady through the morning and midday period at 4 oktas.
(c) Average wind speed at 10 metres (height of anemometer) is 4 m/s.

Step 1. Estimate the incoming solar radiation R.
From Figure 1 read off R_0 appropriate to 0–1 oktas cloud for the month and time of day.
In the example $R_0 \approx 68$ mW/cm^2 for July, $T = 14$ GMT.
Modify R_0 according to the cloud amount, using Figure 2, to give R.
Example: Cloud is 4 oktas, R_0 is 68, which gives R as 48 mW/cm^2.

Step 2. Estimate the ratio of the geostrophic and 10-metre winds, V_g/u_{10}. If u_{10} is known, then Figure 3 gives V_g/u_{10} in terms of R (found from Step 1) and u_{10}.
If u_{10} is unknown but an estimated value of V_g is obtainable from a synoptic chart, then Figure 4 may be used to give u_{10} and V_g/u_{10}. If both u_{10} and V_g are known directly then this step may be omitted or used simply as a check. Clearly in difficult topographical situations where our scheme may be suspect, direct estimates of V_g and u_{10} may be preferred.
In the example $u_{10} = 4$ m/s,
From Figure 3 the value of V_g/u_{10} appropriate to $R = 48$, $u_{10} = 4$ is:

$$\frac{V_g}{u_{10}} \approx 1{\cdot}6.$$

With significant curvature of the air trajectory, V_g should be replaced by the gradient wind following standard procedures.

Step 3. Estimate the depth of the boundary layer, i.e. where the 'free-stream' wind is first achieved.
If a significant synoptically induced inversion exists, this provides an *upper* limit to the boundary-layer depth. Figure 5 gives the depth in the absence of any such inversion or when the inversion is higher than that given by the Figure.
Start with the time of day in the top right-hand box; move upwards to meet the appropriate month curve; move left into the top left-hand box to meet the appropriate cloud-amount curve; move down to the bottom left-hand box to meet the u_{10} curve and finally move to the right and read off the estimated value of boundary-layer depth, h. The 'path' taken for the Example is indicated by the dashed line and yields an estimated $h = 1080$ metres.

Step 4. Estimate the wind profile.
To enter Figure 6, the two parameters V_g/u_{10} and h, found above, have to be known.
In the example $\frac{V_g}{u_{10}} = 1{\cdot}6$ and $h = 1080$ m.
The profile has to be interpolated between the curves shown.
In our specific example the profile lies between those given for $V_g/u_{10} = 1{\cdot}5$ and $1{\cdot}75$, and following the 'tails' up to $h = 1000$ m (approximately).

The values of u_z/u_{10} which may thus be estimated are shown in Table I.

TABLE I–ESTIMATED VALUES OF u_z/u_{10}

z *metres*	V_g/u_{10} =	u_z/u_{10} 1·5	1·75	1·6*	u_z* *m/s*
1		0·78	0·72	0·76	3·0
10		1	1	1	4·0
40		1·11	1·19	1·14	4·6
100		1·22	1·33	1·27	5·1
200		1·28	1·45	1·35	5·4
500		1·42	1·64	1·52	6·1
1000		1·50	1·75	1·60	6·4

* Appropriate to the example

Step 5. The corresponding wind profile over the city can be inferred using the dashed lines on Figure 6. These should only be taken down to within two building-top heights above ground. Below that wind speeds are very variable and are strongly influenced by individual buildings or arrays of buildings.

In the example the winds at 1 m and 10 m cannot meaningfully be defined. At 40 m the average wind is expected to be 4·1 m/s, which is less than the corresponding rural-site speed by 0·5 m/s. At 100 m and above the speed is hardly affected unless the town extends for more than a few kilometres upwind.

The thermal wind. In previous sections any variation of the geostrophic wind with height through the boundary layer has been neglected. However, in many situations this is not justifiable largely because horizontal temperature gradients result in changes in the horizontal pressure gradient with height.

Four simplified situations may be considered (see Figure 7). Situations (a) and (b) result primarily in a change of geostrophic wind *direction* with height

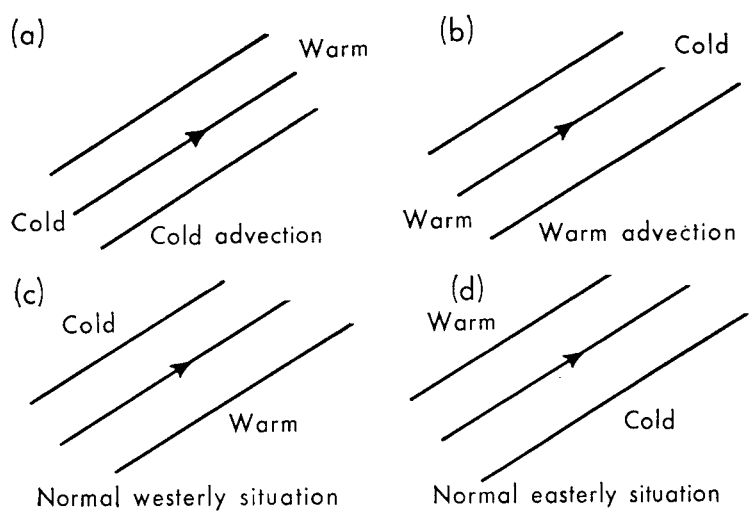

FIGURE 7—THE FOUR SAMPLE SITUATIONS

and we will not concern ourselves with these further. Situation (c) results in an increasing V_g with height whereas in situation (d), V_g decreases with height. The magnitude of these changes is given by

$$\frac{\partial V_g}{\partial z} = -\frac{g}{fT}\left[\frac{\partial T}{\partial y}\right]_p,$$

where strictly $\partial T/\partial y$ is taken normal to the isobars but within a constant pressure surface. Usually this may be approximated by $\partial T/\partial y$ in the *horizontal*, normal to the isobars with an error which is usually well under 1 m/s in $[V_g(z = 1000\text{ m}) - V_g(z = 0)]$.

Since the difference in V_g between the surface and the top of the boundary layer is of primary importance, a representative $\partial T/\partial y$ appropriate to the whole depth of the boundary layer has to be estimated. Unfortunately screen temperatures (at approximately 1·5 m) are not very representative of the mean temperature in the whole layer. Consequently some adjustment has to be made allowing for heat flux and wind speed and by using the conclusions of similarity theory which give typical temperature profiles as a function of stability and height. These factors are employed to give the potential temperature difference between the screen and $z = 100$ m in terms of R (the incoming solar radiation) and the wind at 10 metres. It will be assumed that the implied temperature at 100 metres yields the required representative temperature of the layer.

Probably an adequate procedure to estimate the thermal wind in the absence of radiosonde data is then to select two well-sited stations lying across wind and one or two hundred kilometres apart, take their screen temperatures, adjust them to 100 metres (using Figure 8) and take the station difference.

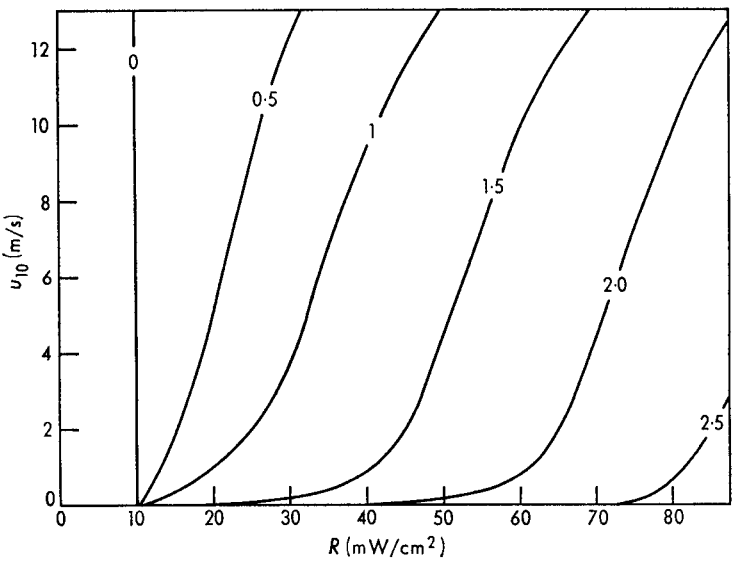

FIGURE 8— CONTOURS OF θ(1·5)–θ(100)

If we denote the temperatures at the two stations by suffixes A and B, and let the stations be n hundred kilometres apart, then define

$$\Delta_{1000}T \equiv \frac{T_B - T_A + \delta\theta_A - \delta\theta_B}{n},$$

where

$$\delta\theta = \theta(1{\cdot}5) - \theta(100).$$

The difference in the geostrophic wind between 1000 metres and the surface is then

$$\Delta V_g \approx 3{\cdot}3\Delta_{1000}T \text{ in United Kingdom latitudes.}$$

Given that the depth of the mixing layer is not 1000 metres but h metres the change in geostrophic wind speed through the layer is simply

$$\Delta_h V_g = \frac{h}{1000}\cdot \qquad \equiv 3{\cdot}3\,\Delta_h T,$$

defining $\Delta_h T$. The magnitude of $\Delta_h T$ is given by Figure 9. The conclusion of this simplified approach is that the magnitude of the geostrophic wind at the top of the mixing layer, h, in terms of u_{10} is given in terms of stability (as in the earlier sections) modified by an additional increment $\Delta_h V_g$,

$$\text{i.e. } V_g(z = h) = V_g(z = 1 \text{ m}) + \Delta_h V_g,$$

remembering that $V_g(z = 1 \text{ m})$ is a function of u_{10}, z_0 and R. The effect of $\Delta_h V_g$ is therefore to modify the ratio V_g/u_{10} used on page 249. Figure 10 shows how this modified ratio can be found very easily. It is immediately obvious that V_g/u_{10} can now lie outside the comparatively narrow range, 1·5 to 2, determined by stability alone.

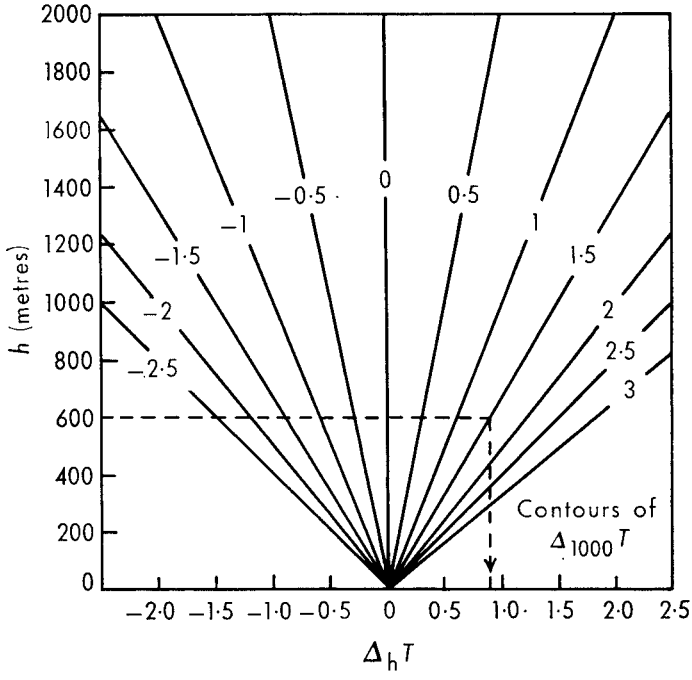

FIGURE 9—DETERMINATION OF $\Delta_h T$

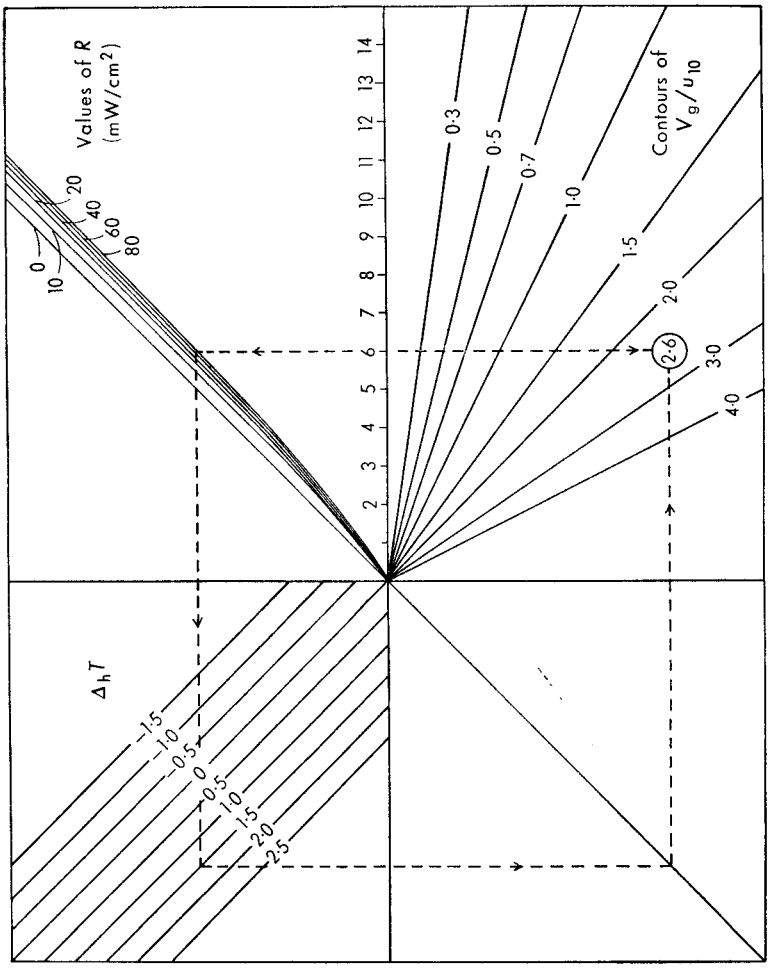

FIGURE 10—NOMOGRAM FOR DETERMINING V_g/u_{10}

Figure 11 shows two sample profiles when the thermal wind effect is quite marked; the one on the left corresponds to an enhanced V_g due to *cold* air to the left of the airstream whilst the one on the right shows a nearly constant wind with height arising from *warm* air to the left of the airstream.

Plotted in this way, profiles are readily constructed. The following constraints and steps may be used:

(a) $u_z/u_{10} \equiv 1$ at $z = 10$ m.

(b) At $z = 1$ m over grass $u_1/u_{10} \approx 0{\cdot}75$ with a gradient which if extrapolated up to $z = 10$ m would give a velocity ratio of $1{\cdot}4$.

(c) The upper part of the profile is first approximated by a straight line that passes through 0·86 at 10 metres and V_g/u_{10} at $z = 1000$ m. This is then modified by smoothly running from the straight line into V_g/u_{10} at $z = h$, with $\partial u/\partial z = 0$ there, as shown in the several examples.

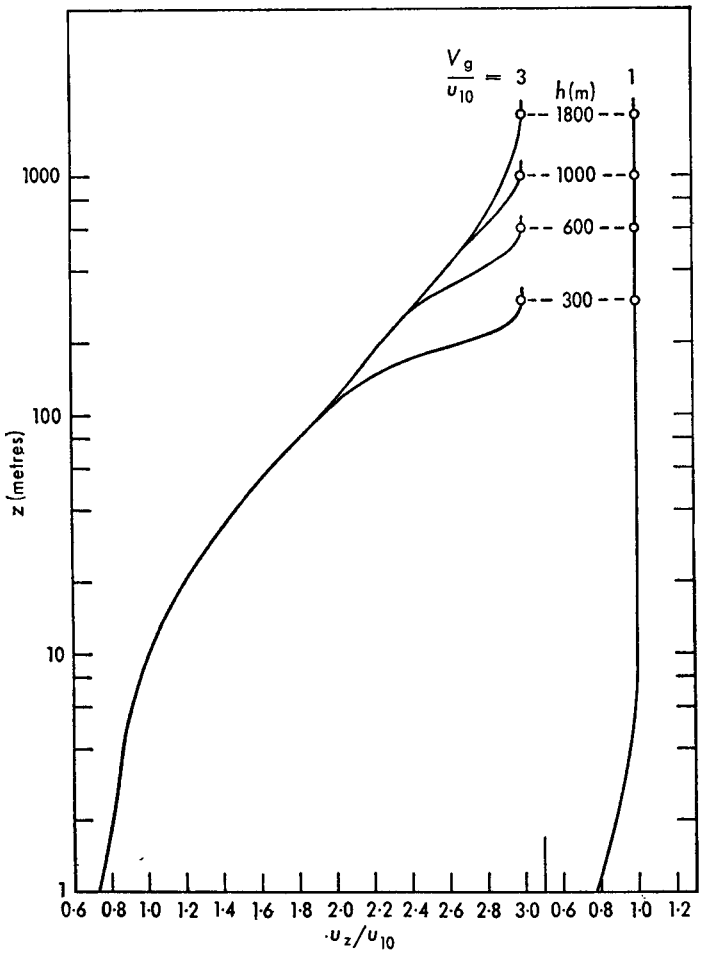

FIGURE 11—TWO EXAMPLES OF WIND PROFILES STRONGLY AFFECTED BY THERMAL WINDS

Both examples are profiles at meteorological stations.

(d) Finally a smooth profile is constructed linking the parts and subject to all the constraints in (a) to (c).

This rather bold approach must inevitably involve errors, but since the constraints are numerous, these must be relatively quite small. The effect of stability on these 'mixed' profiles therefore must be most pronounced in determining V_g/u_{10}, and the shape otherwise is not seriously affected.

REFERENCES

1. SMITH, F. B.; Boundary layer profiles in unstable conditions. London, Meteorological Office, 1969. (Unpublished, copy available in the Meteorological Office Library, Bracknell).
2. SMITH, F. B., CARSON, D. J. and OLIVER, H. R.; Mean wind-direction shear through a forest canopy. *Boundary Layer Met, Amsterdam*, **3**, 1972, pp. 178–190.
3. SMITH, F. B. and JEFFREY, G. H.; The prediction of high concentrations of sulphur dioxide in London air. London, Meteorological Office, 1971. (Unpublished, copy available in the Meteorological Office Library, Bracknell).
4. BUSINGER, J. A.; Transfer of momentum and heat in the planetary boundary layer. Proceedings of a symposium on Arctic heat budget and atmospheric circulation. The Rand Corporation, Santa Monica, California, 1966, pp. 305–332.
5. DYER, A. J. and HICKS, B. B.; Flux-gradient relationships in the constant flux layer. *Q J R Met Soc, London*, **96**, 1970, pp. 715–721.
6. CARSON, D. J.; The development of a dry inversion-capped convectively unstable boundary layer. *Q J R Met Soc, London*, **99**, 1973, pp. 450–467.
7. SMITH, F. B.; A scheme for estimating the vertical dispersion of a plume from a source near ground level. Brussels, NATO Committee on the Challenges of Modern Society. Proceedings of the Third Meeting of the Expert Panel on Air Pollution Modeling, Paris, Oct. 2–3, 1972, Brussels, 1972, Chap. XVII, pp. 1–14.

551.557.37: 551.577.61

A MEMORABLE RAINFALL EVENT OVER SOUTHERN ENGLAND (PART I)

By PAULINE M. SALTER and C. J. RICHARDS

Summary. During the period 14–16 September 1968 parts of southern England experienced a memorably heavy fall of rain and substantial flooding occurred in places; the rain system was particularly intense over the south-east during the 15th. From a meteorological analysis of the situation it appears that the dominant mechanism governing the precipitation over the south-east was a pronounced convergence zone in the lower troposphere, overlaid at upper levels by a strong positive vorticity advection field operating within a narrow zone of marked horizontal wind shear. This system became slow moving on the 15th and, within it, a low-level inflow of potentially unstable, moisture-laden air is envisaged as leading to the 'dumping' of a heavy fall of rain over a relatively small area.

Introduction. Between 14 and 16 September 1968 parts of southern England experienced an unusually heavy and prolonged rainfall that resulted in extensive flooding in the south-east. Headlines appearing in the national Press on the 16th, following the event, were vivid in their description and may be recalled: 'The Great Deluge—Garden of England is a Paddyfield' (*Daily Mail*), 'Floods Devastate South—Hundreds of homes evacuated' (*Daily Telegraph*), 'September in the Rain' (*Daily Express*). In papers by Bleasdale[1, 2] this rainfall has been compared with other exceptional rainfall events in the United Kingdom. The purpose of this paper is to describe the sequence of events and the rainfall distribution and, from available data, to offer some explanation for the weather experienced in the light of the meteorological situation prevailing at the time.

Surface analysis and weather sequence. Two rain systems affected southern England during the period 14–16 September and it was the second of these systems that precipitated the memorably heavy fall over south-east England; both systems were associated with a slow-moving depression in the vicinity of the Bay of Biscay. The first rain belt, characterized by vigorous thundery activity, moved northwards across south-west England during the morning of the 14th, reaching the London area by afternoon. The second, and major rain-producing system, developed over northern France and the English Channel during the evening of the 14th and moved slowly north towards the Channel coast of south-east England on the 15th.

Weather over much of the British Isles had been dominated during the first half of the preceding week by a large area of high pressure over Scandinavia. By the 13th a rather slack pressure gradient was covering the U.K. A slow fall in pressure set in over and to the south-west of the British Isles during the 13th and accelerated over the south-west during the evening, and a depression with central pressure of a little under 1000 mb formed off Brest by midnight on the 14th (see Figure 1(a)). Thundery rain and thunderstorms broke out over Brittany and the South West Approaches accompanying this development, and extended slowly north-eastwards over Cornwall and Devon in association with a cold occlusion. A noticeable feature of this system was the vigorous electrical activity associated with it, as registered in the form of atmospheric reports (SFLOCS). During the morning of the 14th the trough moved northwards over southern England, storms on and ahead of the trough triggering off very high repetition rates of SFLOCS in places, and by midday the thundery activity had transferred into the south Midlands, reaching south-east England and East Anglia by afternoon. A clearer, rather unstable south-westerly airflow behind the trough brought drier conditions into extreme southern counties during the morning. During the afternoon the trough became slow moving from the Bristol Channel to the Thames Estuary, and thundery activity started to die out.

The development of the second system was heralded by a general fall in pressure over central France during the afternoon. This extended northwards in the evening, sharpening and rejuvenating the broad trough of low pressure then lying over the English Channel. The surface wind backed and strengthened north-easterly over the British Isles, promoting the development of a marked trough and zone of convergence over the Channel east of Cherbourg later on the 14th (Figure 1(b)). Renewed rain and thunderstorms broke out over France during the afternoon, drifted slowly north over the Channel in the evening and reached Portland Bill and the Isle of Wight shortly after 00 GMT on the 15th. The rain subsequently spread over central southern England and south-east England, south of the Thames. By 06 GMT on the 15th the depression had drifted southwards over Biscay, extending a broad trough north-eastwards over the Cherbourg peninsula and the Dover Straits. The axis of this trough, marking the main convergence zone, transferred slowly northwards over central Kent, and remained slow moving in a north-east to south-west direction during the morning and afternoon, the strong north-easterly airstream to the north of the trough contrasting markedly with the slack southerly flow to the south (Figure 2(a)). Lying south-east of the trough axis, the extreme east of Kent and Sussex escaped the prolonged heavy rain that was affecting places to the north and west. Though thunderstorms were quite extensive within the

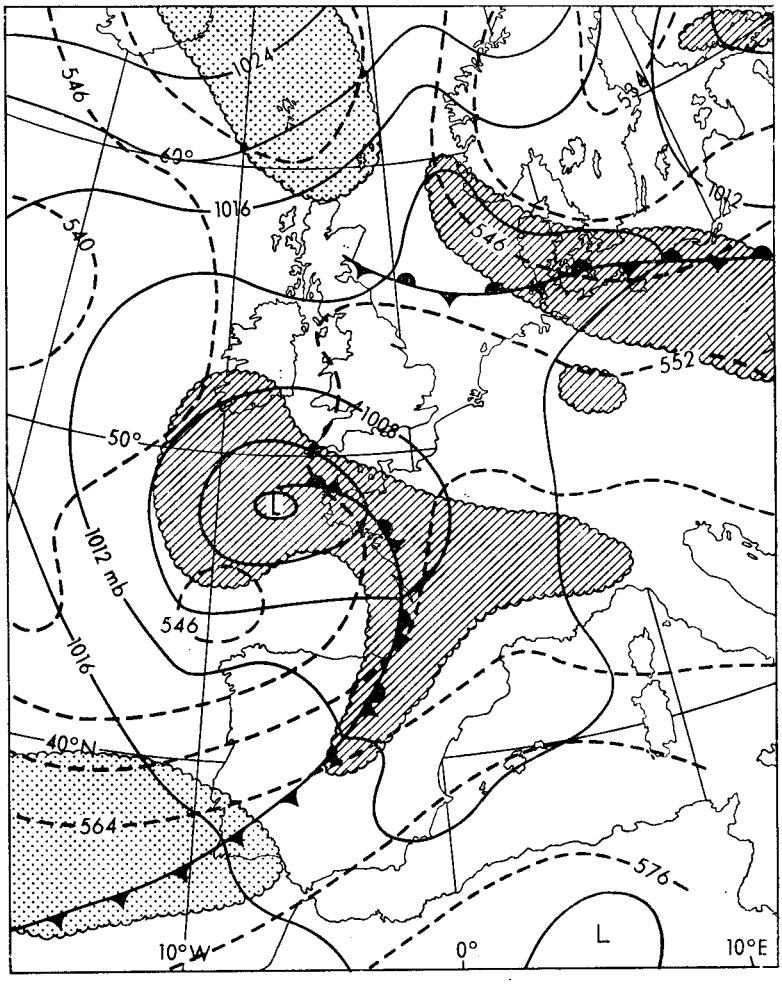

FIGURE I—SURFACE ANALYSIS AND 1000–500-MILLIBAR THICKNESS, 14–16 SEPTEMBER 1968

(a) 00 GMT, 14 September 1968. Thickness values are in geopotential decametres. Hatching shows wet air at 700 mb (dew-point depression < 2 degC). Stippling shows dry air at 700 mb (dew-point depression > 20 degC).

convergence zone during the morning, the electrical activity (as observed in SFLOC reports) was by no means as intense as it had been over central southern England the previous day.

A temporary improvement was occurring south of the Thames by early afternoon of the 15th, but renewed heavy rain broke out over north Kent, Essex, and Suffolk during the afternoon as a small depression formed within the convergence zone over the Thames Estuary. This depression drifted south-westwards over west Kent, returning heavy rain to parts of Kent and Surrey later in the afternoon (Figure 2(b)), but it disappeared as a separate entity near the south coast during the evening. The rain area extended slowly northwards over East Anglia, precipitating continuous moderate or heavy rain here till 03 GMT on the 16th. It also moved over the south Midlands but rain here was much weaker in

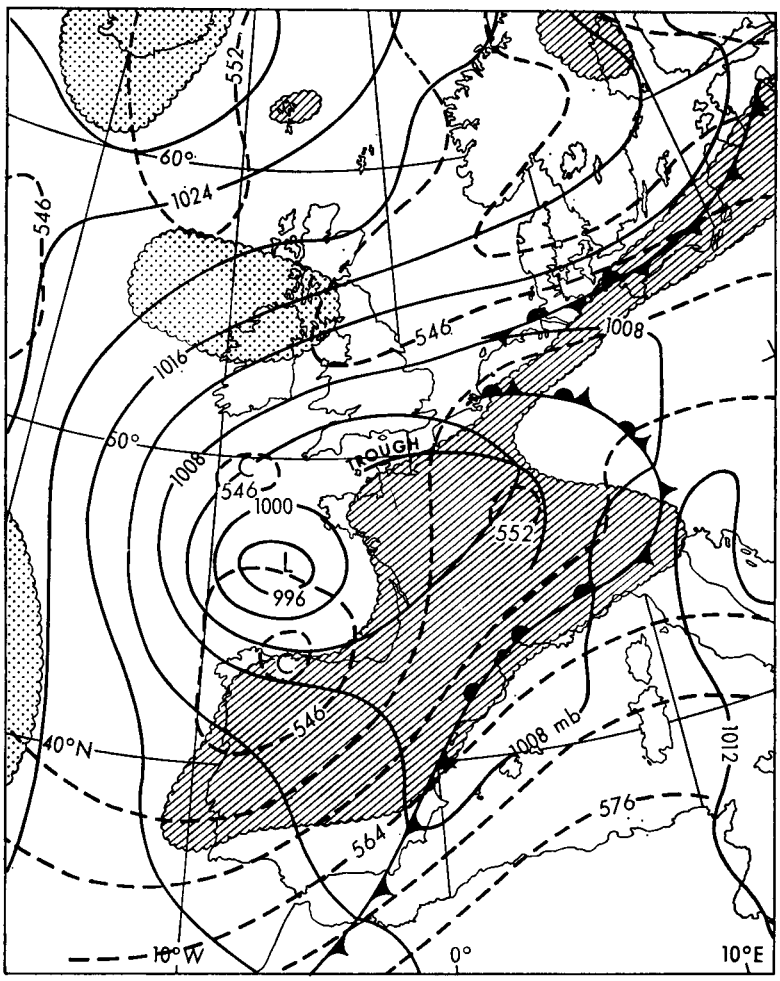

FIGURE 1—*continued*

(b) 00 GMT, 15 September 1968. Thickness values are in geopotential decametres. See also notes under Figure 1 (a)

intensity compared with that nearer the trough. During the evening of the 15th the axis of the trough drifted slowly westwards over the south-east allowing the clearer, drier conditions behind it to spread over Surrey, Kent and Sussex. A further small depression formed in the trough off the Norfolk coast by midnight on the 16th, and drifted over Norfolk, disappearing south of Cambridge by 07 GMT, but at the same time, displacing the main zone of convergence westwards over East Anglia, which it weakened considerably. By midday on the 16th the depression over Biscay had moved over France and degenerated into a shallow, low complex system.

Rainfall distribution. On 14 September rainfall totals in excess of 10 mm were recorded over the area of south-east and central southern England south of a line from Cheltenham to Colchester. The heaviest totals recorded on this

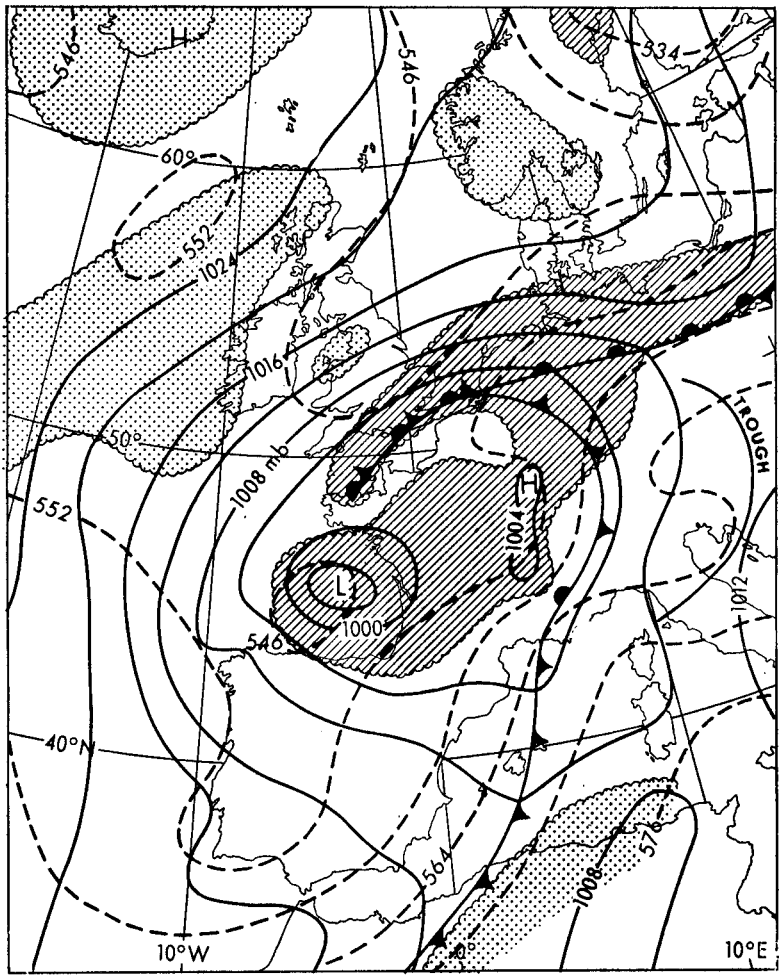

FIGURE 1—*continued*

(c) 12 GMT, 15 September 1968. Thickness values are in geopotential decametres. See also notes under Figure 1(a).

'rainfall day' (in the 24 hours from 09 GMT on the 14th to 09 GMT on 15th) were in a belt running north-eastwards from the east Hampshire border to just east of Maidstone in Kent. Several point falls greater than 100 mm were recorded near Tonbridge and Maidstone. A parallel belt of heavy falls from Croydon to Maldon in Essex had point falls over 90 mm but none in excess of 100 mm.

Rainfall totals in excess of 10 mm covered a wider area on 15 September;* most of the area south-east of a line from Weymouth to Spalding, including the whole of East Anglia, had more than 25 mm. Again the belts of heaviest rainfall ran in a south-west to north-east direction. The widest belt with totals greater than 50 mm, from Winchester to the Thames Estuary, including Clacton in Essex and Herne Bay in Kent, was approximately 50 km wide and had seven centres with recorded rainfall totals of more than 100 mm. These

*In this section dates refer to the 'rainfall day'.

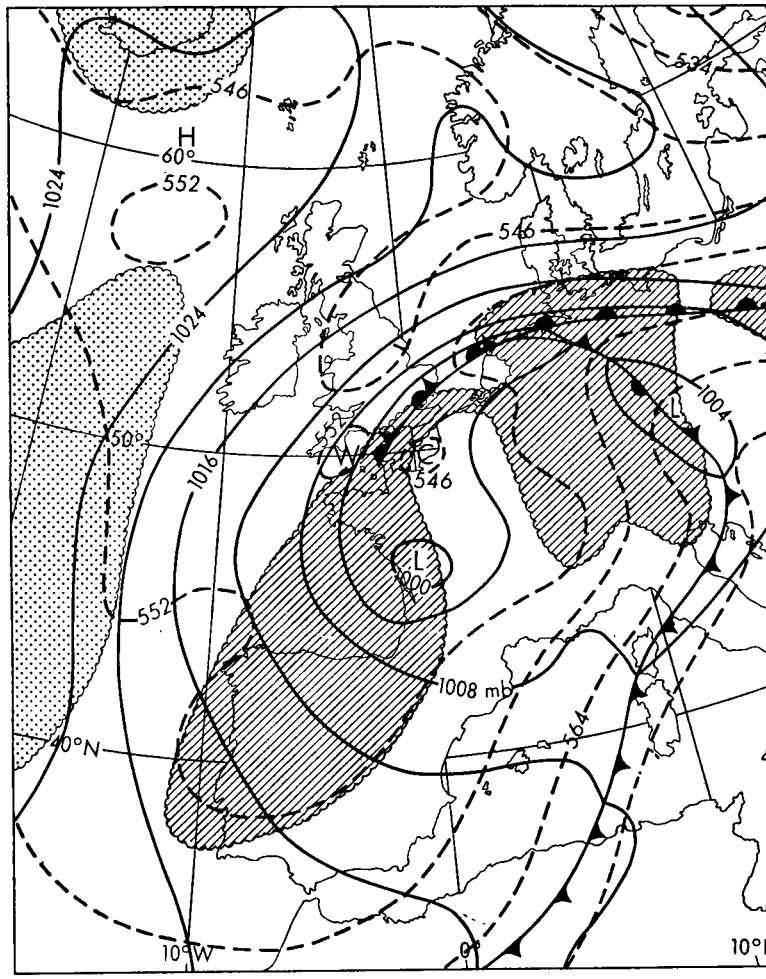

FIGURE 1—*continued*

(d) 00 GMT, 16 September 1968. Thickness values are in geopotential decametres. See also notes under Figure 1(a).

included the highest totals recorded for the rainfall day, 129.5 mm at Bromley in Kent and 123.7 mm and 124.5 mm at Godstone in Surrey. The second belt with totals greater than 50 mm was narrower, 15–25 km, over most of its length from Beaconsfield in Buckinghamshire widening to about 50 km as it crossed Norfolk and Suffolk to the coast with Great Yarmouth on the axis. Although a large part of this belt had recordings of more than 75 mm, there were only five reports of more than 100 mm.

The combined distribution for these two days from 09 GMT on 14 September to 09 GMT on 16 September (Figure 3) shows the area of heaviest falls from Hampshire, across north Sussex, Surrey and Kent and across the Thames to Essex. The highest two-day totals were reported in Essex—201.4 mm at Marsh Farm Sewage Works and 200.9 mm at Stifford Pumping Station—in the Tilbury–Purfleet area. (Other reports are given in Table I.) In these two days

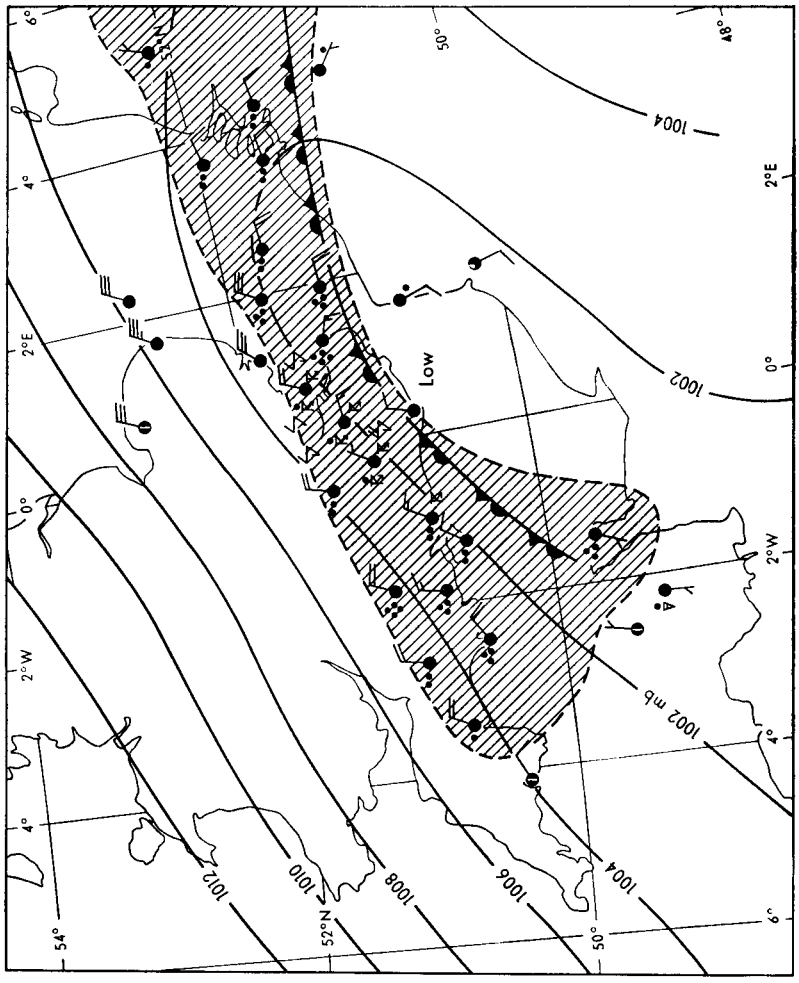

FIGURE 2—SIGNIFICANT WEATHER OVER SOUTHERN ENGLAND ON 15 SEPTEMBER 1968

(a) 09 GMT thunderstorm location reports (SFLOCS) are included. Shading shows the rain area.

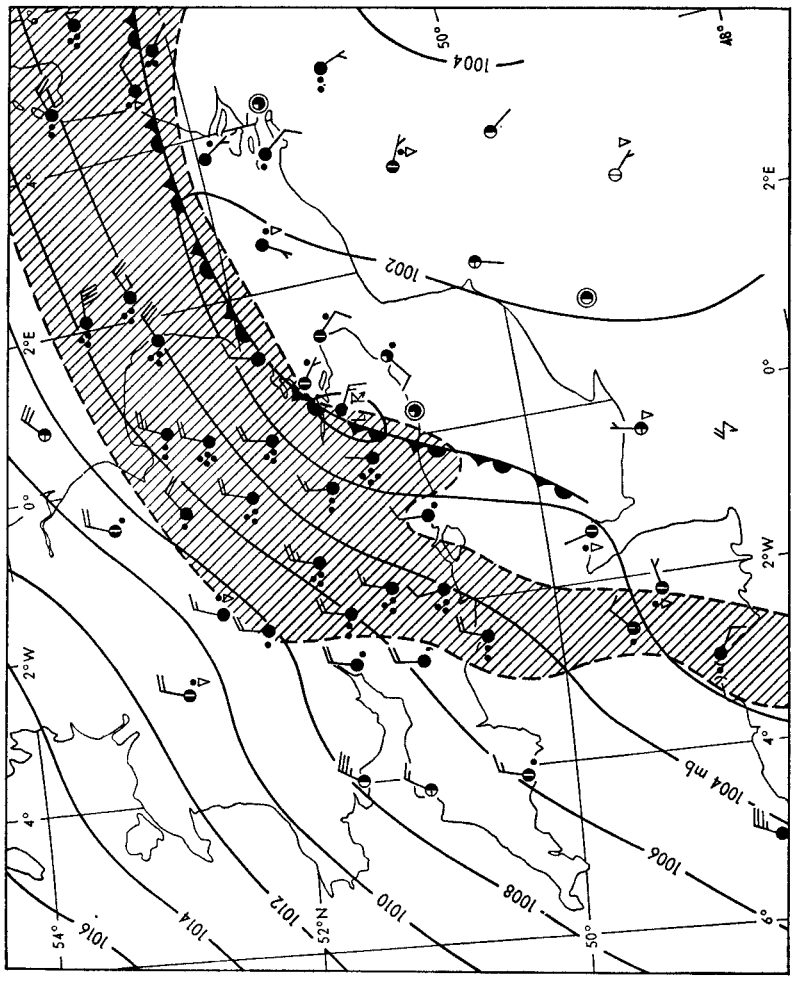

FIGURE 2—*continued*
(b) 18 GMT
Shading shows the rain area.

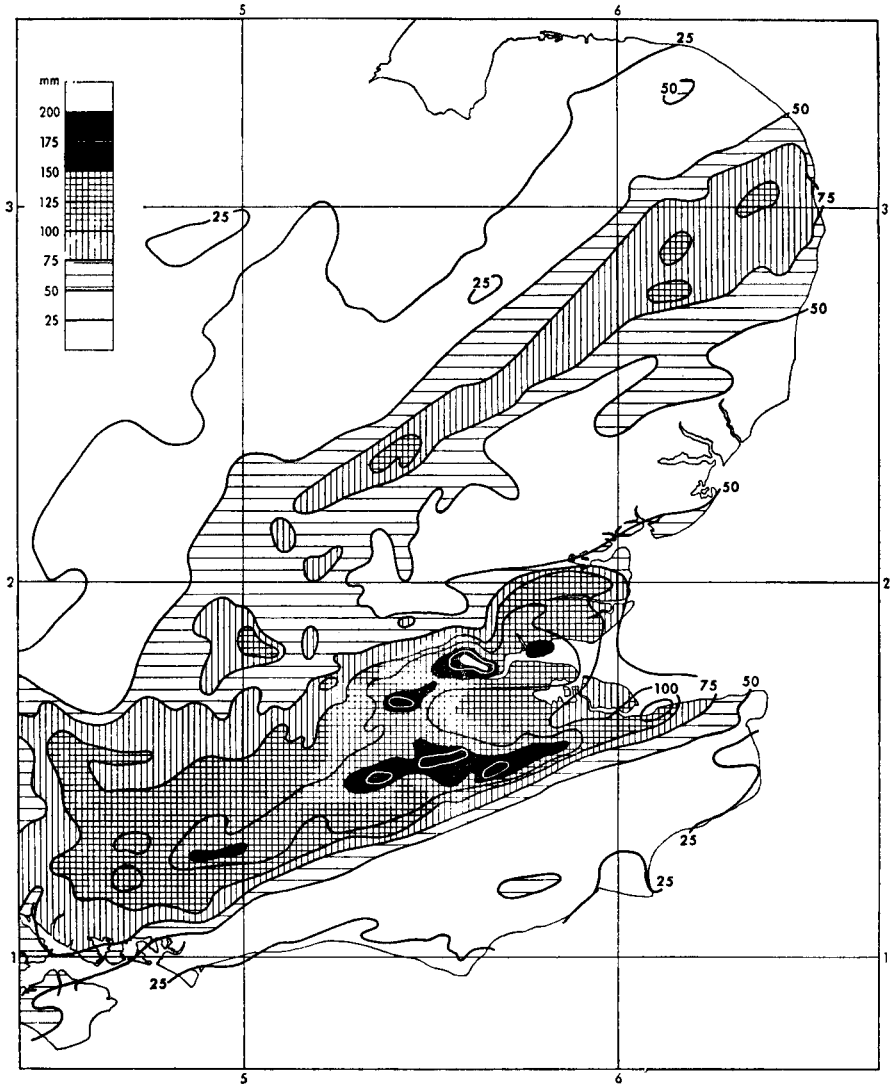

FIGURE 3—TOTAL RAINFALL FOR 14–15 SEPTEMBER 1968
National Grid Lines are shown at 100-km intervals.

most of south-east England and East Anglia had more than 5 per cent of its average annual rainfall. Part of Kent and Surrey, about 450 km^2, and an area of about 750 km^2 along the Thames Estuary had more than 20 per cent of their average annual rainfall. The highest percentages for the two days were in Essex at the two stations recording the highest rainfall totals with 39·0 and 39·7 per cent respectively. A further small amount of rain fell in the area on 16 September but totals were mainly less than 10 mm and were almost negligible compared with the amounts on the previous two days.

Autographic records show few intense short-period falls during the two days but do show that most of the two-day total of rain fell in 24 hours or less,

spanning the two rainfall days. The Broadfield, Crawley, chart shows the main rainfall beginning between 05 and 06 GMT on the 15th and continuing steadily until 13 GMT followed by slight rain for about 5 hours. At 18 GMT it began to rain steadily again and this lasted for 3 hours. This was a fairly typical pattern for stations in Kent and Surrey. North of the Thames the chart for Basildon shows two storms starting at 1630 GMT and 22 GMT on the 14th and this was followed by periods of slight rain until the end of the rainfall day. On the 15th it rained steadily for $5\frac{1}{2}$ hours from 10 GMT with further outbreaks of rain after 20 GMT. It was the storms of the 14th in this area which gave the more intense short-period falls. Across East Anglia most of the rain fell on the 15th starting between 14 and 15 GMT and continuing for 8 to 10 hours. This rain was generally less intense than that which occurred in Kent and Surrey earlier in the day.

Rainfall on previous days. Rainfall for the first 13 days of September was generally less than 50 mm and over quite a large part of the area it was less than 25 mm. Rain fell over the whole area during the first few days, but from the 5th to 9th inclusive most parts were dry. Rain was widespread over the area on the 10th but amounts were generally low. The 11th was dry over much of the area, but a few places in East Anglia recorded between 25 mm and 35 mm. The next two days were dry except for parts of Kent and Sussex. As a result of this, the soil moisture deficit, which on the 11th ranged from 10 mm to 100 mm, was quite large over most of the area.

Flooding and damage. Serious and widespread flooding occurred over Kent, Surrey and parts of Essex, Hertfordshire and Suffolk with localized flooding in many other parts of the area. In general, rivers reached their peak (maximum height) on the 16th and the water continued to spread on the 17th causing disruption to all forms of communication and many thousands of pounds' worth of damage.

The flow in the lower reaches of the River Mole was about four times that of January 1955 which was itself the highest recorded between 1930 and 1955. In Sussex at Park Mound the River Arun rose 5·2 m in 24 hours, from almost zero flow to the highest level ever recorded, and on the Rother the highest level previously recorded at Fittleworth was exceeded by 0·3 m. On both of these rivers and on many others the significant feature was the extra rainfall on the evening of the 15th. By the River Stour in Suffolk the flood was comparable with that of 1947. In the Kent River Authority area, flooding in the valleys of the Rivers Darent, Cray, Eden, Eden Brook and Bourne was far worse than any previously recorded. Besides these valley floods a great deal of flooding occurred remote from the rivers and before the rivers overflowed. The flow of a number of rivers and streams had to be estimated because the gauging stations were either flooded or bypassed by the flood waters.

The total area of land flooded, excluding the Sussex River Authority area for which information is not available, was estimated as 220 km^2 of which more than 100 km^2 were in the Kent River Authority area and 60 km^2 in the Thames Conservancy area. In this latter region it was the area flooded by just three tributaries of the Thames, the Mole, Wey and Loddon. The figure given for the Kent River Authority area includes 44 km^2 of marshland. Again excluding the Sussex River Authority area, almost 21 000 properties were flooded. Over 14 000 of these, of which 10 000 were residential, were in the area of the Thames

Conservancy, mainly in the valleys of the Mole and the Wey. It is reported that one factory alone suffered a loss of £500 000 including damage and loss of production.

A number of roads were impassable for varying lengths of time including the A 23 at Horley and Gatwick, the A 217 at Sidlow, the A 24 at Mickleham, the A 3 at the Kingston Bypass, Cobham and the Guildford Bypass, the A 281 at Shalford, the A 244 at Hersham, the A 329 near Reading, the A 23 at Brasted, the A 21 at Darent and the A 2 at the confluence of the Rivers Cray and Shuttle. At Tonbridge on the 15th all roads northwards were impassable owing to local flooding. Several bridges collapsed and others were damaged by the volume of water rushing under and round them. More details of damage are given in Table II.

Total cost of damage caused by the exceptionally heavy two-day rainfall of 14 and 15 September 1968 is impossible even to estimate. The loss of crops on agricultural land, and the damage to roads and bridges, and to public and personal property cannot even be listed completely.

TABLE I—HIGHEST RECORDED RAINFALL MEASUREMENTS

Station number		National grid reference	Total rain *mm*
14 *September* 1968			
294630	Hildenborough	TQ 51 571488	106·2
295005	Hadlow College	TQ 51 628497	113·0
295010	Hadlow Sewage Works	TQ 51 631491	114·3
297727	Brenchley Gardens, Maidstone	TQ 51 759561	107·7
297722	Mill Street, Maidstone	TQ 51 761555	110·5
290007	Cross Ness, Erith	TQ 51 485809	97·5
237466	Stifford Pumping Station	TQ 51 590802	85·1
236974	Marsh Farm Sewage Works, Tilbury	TQ 51 654756	83·3
235389	Basildon Sewage Works	TQ 51 737908	89·7
235519	Wickford	TQ 51 772921	99·1
15 *September* 1968			
288687	Bromley	TQ 51 399693	129·5
293572	Godstone Sewage Works	TQ 51 365505	123·7
292953	South Godstone Sewage Works	TQ 51 363478	124·5
291253	Priory Gardens, Orpington	TQ 51 465666	121·9
14/15 *September* (48-h totals)			
237466	Stifford Pumping Station	TQ 51 590802	200·9
236974	Marsh Farm Sewage Works, Tilbury	TQ 51 654756	201·4
236632	Canvey Island Pumping Station	TQ 51 800828	155·2
284974	Earlswood Sewage Works	TQ 51 275483	151·1
293572	Godstone Sewage Works	TQ 51 365505	168·4
297340	East Farleigh Lock	TQ 51 735535	162·3
297727	Brenchley Gardens, Maidstone	TQ 51 759561	157·7
297347	Barming Water Works, Maidstone	TQ 51 735548	153·4
293953	South Godstone Sewage Works	TQ 51 363478	189·8
288687	Bromley	TQ 51 399693	190·5
290200	Sundridge Pumping Station	TQ 51 489556	160·8
290060	Erith Sewage Works	TQ 51 523777	154·4
290070	Westwood Pumping Station, Surrey	TQ 51 425541	150·1
290241	Chevening Gardens, Sevenoaks	TQ 51 484577	162·6
290412	Stone Street, Kent	TQ 51 572549	176·2
294056	Paines Hill, Limpsfield	TQ 51 412513	157·8
294630	Hildenborough	TQ 51 571488	171·0
295010	Hadlow Sewage Works	TQ 51 631491	165·1
295945	Yalding, Kent	TQ 51 690497	154·4
297707	Hockers Lane Pumping Station, Maidstone	TQ 51 788571	159·6
297455	College Road, Maidstone	TQ 51 757549	165·1

Note: Many of these values were reported in inches and have been converted to millimetres.

TABLE II—FLOOD DAMAGE

Thames Conservancy area

Area flooded

River Mole between Molesey and Horley	21·2 km²
River Wey between Weybridge and Farnham	21·5 km²
River Loddon	18·3 km²

Damage to bridges

River Mole	Betchworth Bridge	Loss of both parapets
	Brockham Bridge	Loss of one parapet
	Boxhill Bridge	Collapse of one arch
	Stoke D'Abernon (rail)	Displacement of girders
	Downside Bridge	Collapse of two arches
River Wey	Brockford Bridge	Collapse of one arch
	Brooklands	Partial collapse of span carrying services
Hoe Stream	Godalming (rail)	Collapse of one span
Cranleigh Waters	Shalford (A 281)	Collapse of arch

Flooding of properties (provisional figures)

Local authority*	Houses	Other premises
Aldershot M.B.	7	1
Chertsey U.D.	200	20–30
Crawley U.D.	150	included
Dorking and Horley R.D.	200	included
Easthampstead R.D.	8	0
Esher U.D.	8000	included
Farnborough U.D.	24	included
Farnham U.D.	220	included
Godalming M.B.	110	10
Guildford M.B.	300	160
Guildford R.D.	170	a few
Hambledon R.D.	400	included
Hartley Wintney R.D.	24	included
Leatherhead U.D.	315	50
Reigate M.B.	200	150
Walton and Weybridge U.D.	2000–2500	included
Wokingham U.D.	1000	not known
Wokingham M.B.	33	2
Wokingham R.D.	70	included

Kent River Authority area

Area flooded

River Medway	26·9 km²
River Bourne	2·6 km²
River Eden & Eden Brook	15·6 km²
River Darent	7·2 km²
River Cray	2·8 km²
River Shuttle	2·3 km²
Warden Bay Drainage	0·3 km²

Marshes

Allhallows, Grain	9·2 km²
Higham Cliffe	24·8 km²
East of Gravesend	3·8 km²
Swanscombe	0·5 km²
Dartford–Stone	2·3 km²
Sea-salter	2·8 km²
Hoo	0·3 km²

* Local Authority areas are as before 1 April 1974. M.B., U.D. and R.D. denote Municipal Borough, Urban District and Rural District.

Properties flooded

	Houses	Others
Westerham	110	3
Brasted	18	0
Sundridge	12	2 including one bridge
Chipstead	61	3
Dunton Green	10	3
Riverhead	4	6
Sevenoaks	some houses	farm buildings
Kemsing	11	farm buildings
Otford	5	one bridge
Shoreham	34	4 + 2 bridges
Eynsford	20	2
Farmingham	6	2
South Darenth	53	0
Dartford	238	258
St Mary's Cray	12	0
Crayford	number not known	—
Edenbridge	140	36
Tonbridge { Hildenborough	362	—
Tonbridge { Barden area	450	152
East Peckham	many houses and industrial properties	
Yalding	40	included
Maidstone	number not known	—
Hadlow	43	15

Essex River Authority area

Area flooded

Tilbury Marshes	2·0 km²
East and West Tilbury Levels	2·0 km²
Mardyke catchment	9·7 km²

Properties flooded

	Houses	Others
Sudbury	1	0
Haverhill	168	—
Keddington	15	included
Sturmer	19	included
Clare and Stoke-by-Clare	13	included
Cavendish	34	included
Long Melford	15	included
Bures	21	included
Cornard	6	included
Stratford St Mary	18	included
Wickford	50	included
Southend	200	1
South Benfleet	30	1
Canvey Island	120	included
Purleigh	4	a few
Hawkwell–Hockley–Rochford	60	—
Fobbing	—	industrial premises
Rainham	40	—
Loxford Water area	20	—
Mayesbrook area	20	—

Lee Conservancy area

Area flooded

Rivers Lee, Mimram, Beane, Rib, Ash, Start	25·6 km²

Properties flooded

	Houses
River Beane upstream of Hertford	104
River Rib upstream of Hertford	140
Bishop Stortford	100
River Lee, Hertford to Hoddesdon	310

Greater London Council area		
Area flooded	Houses	20·0 km²
Properties flooded	3000	

Note: Many of the areas given in this table were supplied in acres or square miles and have been converted to square kilometres.

Part II of this paper will be published in October.

REFERENCES

1. BLEASDALE, A.; The rainfall of 14th and 15th September 1968 in comparison with previous exceptional rainfall in the United Kingdom. *J Inst Wat Engrs, London*, **24**, 1970, pp. 181–189.
2. BLEASDALE, A.; The year 1968, an outstanding one for multiple events with exceptionally heavy and widespread rainfall. *Brit Rainf* 1968, *London* (in press).

REVIEWS

The use of satellite pictures in weather analysis and forecasting, WMO *Technical Note* No. 124, by Ralph K. Anderson, Jerome P. Ashman, Golden R. Farr, Edward W. Ferguson, Galina N. Isayeva, Vincent J. Oliver, Frances C. Parmenter, Tatiana P. Popova, Rance W. Skidmore, Arthur H. Smith and Nikolai F. Veltischev (edited by R. K. Anderson and N. F. Veltischev). 280 mm × 215 mm, pp. ix + 275, *illus.*, Secretariat of the World Meteorological Organization, Geneva, Switzerland, 1973. Price: Sw. Fr. 60.

This publication is a revision of *Technical Note* No. 75, produced as a result of a recommendation of the Commission for Synoptic Meteorology at its fifth session (June–July 1970) that an updated version should be prepared and issued in loose-leaf form to facilitate subsequent updating. A welcome feature of this new version is the collaboration of U.S.S.R. experts and as a result the incorporation of pictures from the COSMOS and METEOR satellites and the addition of many references to work in the U.S.S.R.

As might be expected, the opportunity has been taken to present the whole subject in a more general and comprehensive way than was possible in 1966 when *Technical Note* No. 75 first appeared. Chapter I, 'General characteristics of visible and infra-red images', serves as an introduction and provides essential information on both visual and infra-red images and on the equipment used to produce them. Chapter II, 'Atlas of cloud types, cloud formations and underlying surfaces', presents the necessary information for the practice of picture interpretation. From then on, the emphasis is on the application of satellite data, to weather analysis in extratropical latitudes (Chapter III), to synoptic analysis in the tropics (Chapter IV) and to the estimation of useful meteorological parameters (Chapter V). One of the pleasing new features is the arrangement of pictures close to the appropriate text, making for easier reference.

Many forecasters still do not have direct access to satellite pictures but are dependent on nephanalyses. Nowhere in this publication is any guidance given for the preparation and use of nephanalyses nor indeed any information on the preparation and use of coded satellite information. It is well known that

satellite information has its maximum value when integrated with more conventional data. There is a tendency throughout, particularly in the sections on applications to analysis and forecasting in extratropical latitudes to neglect this aspect and to treat satellite data as existing in isolation. This is surely a mistake, leading inevitably to an over-academic approach. In particular, the section on the use of satellite pictures to forecast the evolution of synoptic-scale disturbances provides forecasting rules derived solely from picture interpretation. Forecasting in extratropical areas is now more dependent on the use of numerical models and it is more relevant to know how satellite information can be incorporated in analyses to best advantage. Some information on this is given in the last chapter. This is obviously a most important subject particularly at the present time when the effect of data shortages on the performance of numerical models is only too evident.

Meteorologists everywhere will welcome this revised version and will look forward to subsequent extensions incorporating wider concepts of the use of satellite pictures in analysis and forecasting.

T. H. KIRK

Partial differential equations of mathematical physics, by Tyn Myint-U. 250 mm × 170 mm, pp. xiv + 365, *illus.*, Elsevier/Excerpta Medica/North-Holland Associated Scientific Publishers, Jan van Galenstraat 335, Amsterdam, The Netherlands, 1973. Price: 43.50 Dfl.

The title is the same as or similar to that of a number of other mathematical textbooks that are available and its contents follow fairly closely the traditional treatment of the subject. After the introduction and derivation of the equations for the physical problems, the canonical forms and general properties of second-order partial differential equations are treated and this leads on to the initial value or Cauchy problem. After a digression to derive the main results in the theory of Fourier series, the method of solution by separation of variables is described and illustrated. The Sturm–Liouville equations and some special functions are included in the chapter on eigenvalue problems. Solution of boundary-value problems in two dimensions with Dirichlet, Neumann and mixed boundary conditions follows. The last three chapters deal with the use of Green's functions to obtain solutions, with integral transforms and with equations in three or more space dimensions.

The contents are selective, and the book cannot rival more comprehensive treatises such as Courant Hilbert. But the selection is well made so that the argument proceeds without too much need for digression. The approach is based on the mathematical problems and their solution, the physical systems in which the equations occur entering only briefly in the initial derivation. The book is therefore not appropriate for readers who are looking for physical insight into the equations or for methods for solving practical problems by numerical methods.

With a text covering such a well-known field the main question that arises is probably 'For what kind of reader can it be recommended?'. Writing as a meteorologist whose mathematics has grown rusty, the reviewer found it suitable for the purpose of reminding him of the mathematical basis of many

problems arising in meteorology. Almost all the important equations from this source are treated, and, from this same point of view, very little of the total content could be considered redundant. I suspect most dynamical meteorologists could read it with considerable profit. For clarity of style and printing the text is admirable. Those with the necessary mathematical background will find it a pleasure to read. There is a wealth of problems of varying difficulty which makes it especially suitable also for students fairly new to the subject.

While, therefore, it can hardly be recommended as essential reading, this book should find a grateful readership among those who are looking for a clear, straightforward and comparatively easy account of the mathematical theory of the standard partial differential equations which occur in physical problems.

A. GILCHRIST

The physics of air–sea interaction, by S. A. Kitaigorodskii. 250 mm × 175 mm, pp. vi + 237, *illus.* (translated from the Russian by the Israel Program for Scientific Translations, Jerusalem), John Wiley & Sons Ltd., Baffins Lane, Chichester, Sussex, 1974. Price: £7.65.

Active research in the field of air–sea interaction now involves a range of topics too broad to be discussed comprehensively in a single textbook. The present monograph is concerned solely with small-scale interactions between ocean and atmosphere and its scope is correspondingly limited, but this restriction in subject matter has given the author enough space to develop some of his ideas in considerable detail. Kitaigorodskii has carried out research in a number of aspects of small-scale processes near the sea surface and he admits that the contents of his book reflect his particular interests; thus, while he has written in most cases with considerable authority, there is inevitably selectivity also, and some imbalance.

The text is divided into three main sections. The first occupies roughly half the book and is concerned with the dynamics of the near-surface atmosphere including vertical turbulence transfers. This part of the book is likely to be of most interest to meteorologists. It begins with an introductory chapter on flow over a solid boundary and follows with descriptions of the changes which result in the flow when the rigid boundary is replaced by the waving sea surfaces. The section concludes with empirical data on the exchange coefficients for vertical transfers of momentum, heat and water vapour, and the effects of departures from neutral density stratification. Of particular interest is the discussion of the complex (and as yet undiscovered) relation between drag coefficient, wind speed and sea state.

The second main section is concerned with ocean waves. Dimensional arguments are used to derive the principal features of spectra of fully developed waves, and of waves after limited fetch or limited duration of wind. A brief description is given of the Miles–Phillips theory of wave development.

The final section deals with vertical mixing processes in the upper ocean. This is probably the least satisfactory part of the book, and Kitaigorodskii himself writes 'The . . . section appears to be premature'. There is a considerable amount of empiricism and while several problems are formulated, few

satisfactory answers emerge, even, for example, when important factors such as existing stratification or time dependence are omitted from discussions of wind mixing.

The translation suffers from a few flaws which careful editing by a micrometeorologist or oceanographer would have eliminated. For example, it is unusual to talk of a 'deep minimum' in the power spectrum of wind velocity (p. 24). The retention of conventional Russian notation hinders easy reading: examples are P for air density and q_θ, W_E for the vertical fluxes of heat and water vapour. However, in spite of the volume's restricted scope and its blemishes it is a welcome addition to the literature of air–sea interaction. The price is no higher than one expects in these inflationary times.

N. THOMPSON

OFFICIAL PUBLICATION

The following publication has recently been issued: *Annual report on the Meteorological Office* 1973, London, HMSO, 1974. Price: £1.10.

The Director-General, in the foreword to his report for the year ending 31 December 1973, highlights the marked increase in demand for meteorological information from industry and the general public. The number of direct inquiries to the Office reached an all-time record of 1.75 million, while another all-time record of 15.5 million calls were made to the Post Office Automatic Telephone Weather Service.

The computer-based forecasts were further refined during the year, but the Director-General stresses the difficulties of maintaining an adequate network of observations, particularly over the oceans, and warns that any deterioration of the network could have an adverse effect on the accuracy of weather forecasts.

Activity in research was maintained at a high level. Work on the development of mathematical models to simulate and perhaps predict the behaviour of the atmosphere on relatively long time-scales continued. Anomalies in sea surface temperatures can have far-reaching effects on the development of weather patterns and one very interesting experiment strongly suggested that an area of abnormally warm ocean off West Africa was an important factor in producing the very cold winter of 1962–63.

The production of nitrogen oxides in the stratosphere by supersonic transport aircraft and their possible effects on ozone concentration at high levels have aroused considerable controversy. Calculations by Meteorological Office scientists indicate that the quantities of nitrogen oxides injected into the stratosphere by nuclear test explosions in the 1950s and 1960s were equivalent to those likely to be produced by 1000 Concordes each flying 7 hours a day. Moreover, analysis of world-wide ozone reports before and after the nuclear explosions fails to reveal any detectable changes in ozone content.

HONOUR

The following appointment to the Imperial Service Order was announced in the Queen's Birthday Honours List, 1974:
Mr H. C. Shellard, Principal Scientific Officer, Met O 3.

OBITUARY

It is with regret that we have to record the death of Mr P. Jenkins, Assistant Scientific Officer, Met O 2, on 31 May, 1974.

THE METEOROLOGICAL MAGAZINE

VOL. 103 NO. 1226 SEPTEMBER 1974

CONTENTS

NOTICES

It is requested that all books for review and communications for the Editor be addressed to the Director-General Meteorological Office, London Road, Bracknell, Berkshire, RG12 2SZ, and marked 'For Meteorological Magazine'.

The responsibility for facts and opinions expressed in the signed articles and letters published in this magazine rests with their respective authors.

Printed in England by The Campfield Press, St. Albans
and published by
HER MAJESTY'S STATIONERY OFFICE

28p monthly **Annual subscription £3.78 including postage**

(16953) Dd. 506683 K16 9/74 ISBN 0 11 722139 2